

Longitudinal Injection Studies for the ESS and SNS

SNS/ORNL/AP TECHNICAL NOTE

Number 001

J. D. Galambos, ORNL

J. A. Holmes, ORNL

D. K. Olsen, ORNL

Oct. 3, 1997

Spallation Neutron Source Project
Oak Ridge National laboratory
PO Box 2009 MS 8218
Oak Ridge TN 37831

Longitudinal Injection Studies for ESS and SNS

I. Introduction

Studies have been started to better understand the differences between injection schemes for the ESS and SNS accumulator rings. These studies consist of performing injection runs with the ACCSIM [1] code for both the ESS and SNS rings. In addition to elucidating differences between the ESS and SNS injection scenarios, this exercise also verifies that ACCSIM reproduces the same basic features seen in the ESS calculations [2]. Some of the relevant parameters for these devices are listed in Table 1. While many of the parameters are similar, a major difference is that ESS injects into a region of dispersion, whereas the SNS does not. Information used in setting up the runs for the ESS was taken from Refs. [2-5]. This memo concentrates mostly on the longitudinal-phase-space aspects of injection.

II. ESS Injection.

The ESS injection process involves simultaneous ramping of the linac beam injection energy, the RF frequency and the RF voltage. These ramps facilitate: (1) painting in the longitudinal space (hence in the X space since injection is at a finite dispersion), (2) keeping the bunch near the center of the bucket, and (3) controlling “arms” which develop in the phase space early in the injection process. This scenario is in contrast to SNS injection, which to date do not incorporate such ramps. Figure 1 shows the ramping scenarios used, reproduced from Ref. [3], and resulting longitudinal phase space distributions predicted by ESS. In order to understand the impact of these ramps, a series of runs was done progressively including each variation. As the ramping of the energy, RF frequency, and RF voltage have a direct effect on the longitudinal distribution, special attention is focused here.

We note that the ESS injection ends at 0.6 msec (i.e. 1000 turns) and the particle tracking continues for another 0.6 msec (1000 turns) because the injected bunch of particles must be held while a second ring is being filled. This is in contrast to the proposed SNS method of extracting the bunch as soon as injection is finished.

II.1 No longitudinal ramping

First we consider a case with constant injection energy of 1.334 GeV, constant RF frequency of 1.67138 MHz and constant RF voltage of 27 kV. Figure 2a shows the longitudinal distribution at four times during the injection process, and the transverse distribution at the extraction time. In this case the longitudinal distribution is symmetric about the synchronous phase $\phi = 0$. An important feature evident in the longitudinal phase space plots is the growth of phase-space “arms”, originating between 500 and 1000 turns. These arms subsequently wrap around the main distribution during the synchrotron motion, extending into the extraction gap and coming close to the separatrix. The arms consist of particles injected early on at large ϕ . As the top and bottom “lobes” of the longitudinal distribution begin rotating, a peak in the longitudinal

distribution develops near $f = 0$ (see turns 500 and 1000). At exactly $\phi = 0$ the confining force from the RF bucket is zero. The space charge potential generated from this gradient in the longitudinal distributions overwhelms the applied RF voltage for the range $-60^\circ \leq f \leq 60^\circ$, causing a growth in $|\Delta E|$ of the “arms” after they cross $f = 0$. The magnitudes of the space charge and RF voltages are shown in Fig. 2b for turn 1000 of this case. The formation of a large space charge at $f \sim 0$ near the end of injection is a ramification of injecting all the particles on a time scale small compared to a synchrotron period. The ends of the initially injected distribution have rotated only about 90° by the time all the particles are injected. This results in a large accumulation of particles near $f = 0$ at the end of injection giving a high space charge there. Later on as the synchrotron oscillation progresses, the longitudinal distribution flattens near $f = 0$ (see turns 1500 and 2000), and there is no more formation of arms. But the arms formed earlier on still exist and must be confined since they have a tendency to rotate into the extraction gap region. The formation and ramification of these arms is discussed further below.

The final transverse distribution is shown also. The spread in the X direction results from the injection into dispersion and the momentum spread. The Y spread results from a closed orbit bump. The ACCSIM results predict about 7.4 foil traversals/particle, consistent with ESS calculations.

II.2 Ramped injection energy

Figure 3 shows results for a similar case as above, but with the injection energy ramped as per Figure 1. The RF frequency is held fixed at a synchronous energy of 1.334 GeV, and the RF voltage is held fixed at the peak value of 27 kV. The general behavior is similar as Figure 2a, but since the injection energy is above the synchronous energy for the RF frequency, the upper half of the distribution rotates faster than the lower half, resulting in a shift of the main part of the distribution towards lower angles (see 1500 turns). Between 1500 turns and 2000 turns, there is a shift of particles to lower energies, and a rebound of the bulk distribution back towards higher phase angles. Also an asymmetric distribution results with the lower arm being larger than the upper arm.

The final transverse distribution is similar to the previous case, except shifted to lower X, since $\langle \Delta E \rangle$ is lower at the final time, except for the tip of the lower arm, which causes the “spray” at higher X near the center of the Y distribution. Also, the foil traversals/particle are ~ 7.9 , similar to the above case.

II.3 Ramped injection energy and RF frequency

Figure 4 shows the longitudinal distribution progression with the additional effect of ramping the RF frequency as per Figure 1. Initially the injection energy is below the RF frequency, resulting in a faster movement of the lower half of the longitudinal distribution (see 500 turns). Subsequent to 500 turns the injection energy is above the RF frequency, but there is less movement of the bulk distribution back towards higher f than the above case. In fact, the upper arm has crossed the separatrix at turn 2000, and become lost. The final transverse distribution is similar to the previous cases and has 7.5 foil traversals/particle.

II.4 Ramped injection energy ,RF frequency, and RF voltage

The final case of the sequence includes ramping of injection energy, RF frequency, and RF voltage as per figure 1, and results are shown in Figure 5. Because of the lower initially applied RF voltage, the synchrotron oscillation starts off slower. The arms which form are smaller, and better confined within the separatrix compared to the previous case. The behavior of the longitudinal distribution is generally similar to that from the ESS calculations, with the exception of the precise movement of the arms. In Figure 5 the arms have not wrapped around the main distribution at the extraction time as much as in Figure 1, resulting in an unacceptable population of the extraction gap. The numerical nuances which affect the arm movement are discussed below. Again, the final transverse distribution is similar to the previous cases and has 7.6 foil traversals/particle.

III Longitudinal Space Charge Calculation Method

The generation and movement of the arms on the longitudinal distribution is due to longitudinal space charge effects. A key component in evaluating the longitudinal space charge is evaluation of the line density gradient, i.e. calculating a smooth quantity from a information resulting from a statistically sampled distribution. In ACCSIM, this “smoothing” is dependent on several assumptions including: (1) number of longitudinal bins , (2) number of digital smoothing passes, and (3) number of particles which are tracked. In all the previous cases, 80 bins, 2 smoothing passes, and 10^4 particles were used. Figure 6 shows the sensitivity of the final longitudinal distribution to changes in these longitudinal smoothing parameters. Increasing the number of particles does not have a big impact on the distribution. However, increase of the number of bins, and use of fewer smoothing passes (160 bins, 10^5 particles, 1 smoothing pass) results in less a filamentation of the main distribution near the ends (i.e. formation of additional smaller arms), which appears to affect the wrapping of the upper arm around the main distribution. It is not clear whether these effects are real or numerical artifacts and additional runs with more particles are needed to resolve this.

IV SNS Injection

IV.1 Nominal scenario

Typically, the formation of the longitudinal arms discussed above, is not seen in SNS injection cases. Longitudinal distributions during a typical injection scenario are shown in Figure 7. For SNS, injection occurs over the entire period in-which particles are held in the ring. While there is a buildup of a peaked line density near $f = 0$ for turns 400-600, less than half the particles have been injected at this time, and the space charge effect is too small to cause arm formation. By the time most of the particles are injected, the density profile is flat in the center, no arms are formed, and there is minimal degradation of the extraction gap. In addition the SNS has 42 kV of peak RF voltage compared to the ESS 27 kV.

IV.2 Faster injection scenario

In order to try and duplicate the formation of the arms with SNS injection we performed some additional calculations. First, we assume that the particles can be injected twice as fast as the base case (i.e. in the first 612 turns), and are subsequently held for another 613 turns. This will simulate the effect of injecting the particles on a time scale closer to the synchrotron oscillation period as per ESS. These results are shown in Figure 8. The behavior is similar as the above case for the first 600 turns. Even though twice as many particles are injected over this period compared to the previous case, the space charge forces are still not strong enough to overwhelm the RF voltage to the degree that arms are formed which wrap around into the extraction gap.

IV.3 Faster injection scenario, Lower RF Voltage

As a final variant from the nominal SNS scenario, we assume that not only is the injection occurring twice as fast, but also that the applied RF voltage is only 21 kV, half the nominal value. For this case, shown in Figure 9: (1) the injection occurs during a fractional synchrotron period similar to ESS, and (2) the applied RF voltage is similar to that in ESS. Because of the lower RF voltage, the synchrotron movement of the bunch is slower than the previous example. Line density peaking near $f = 0$ does not occur until after 400 turns, but at this time there is a sharper peak, resulting in higher space charge voltages. In this case, arms similar to those seen in the ESS cases do form, and ultimately extend into the extraction gap.

Conversely we have calculated that using the ESS injection scheme with a long injection time and more RF voltage results in longitudinal distributions similar to those of the SNS. The arms shown in Figure 1 are the result only of low RF voltage and a fast injection time. From this point of view a two-ring parallel injection scheme which fills the rings simultaneously may be preferred to a series injection scheme which fills the rings sequentially. In addition, the weakness of the dual harmonic and barrier bucket RF systems is apparent for non-uniform longitudinal particle distributions with large space charge forces in the bucket center. With these more complicated RF systems there is more length in the center of the bucket which has a low voltage to confine particles experiencing large space charge forces.

References:

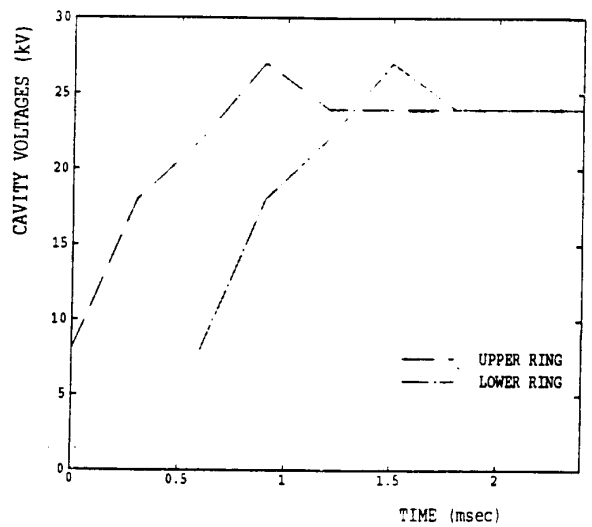
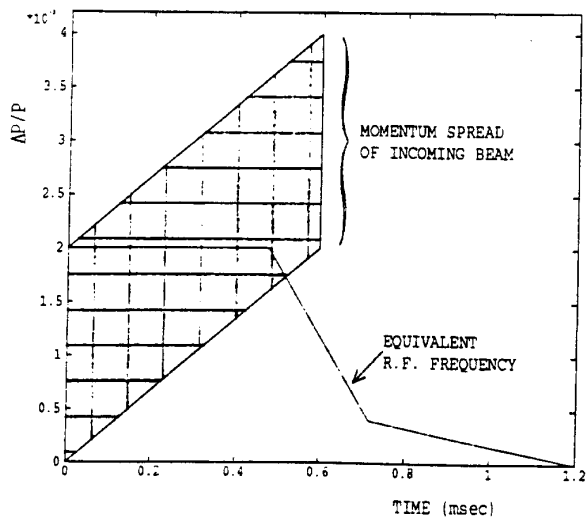
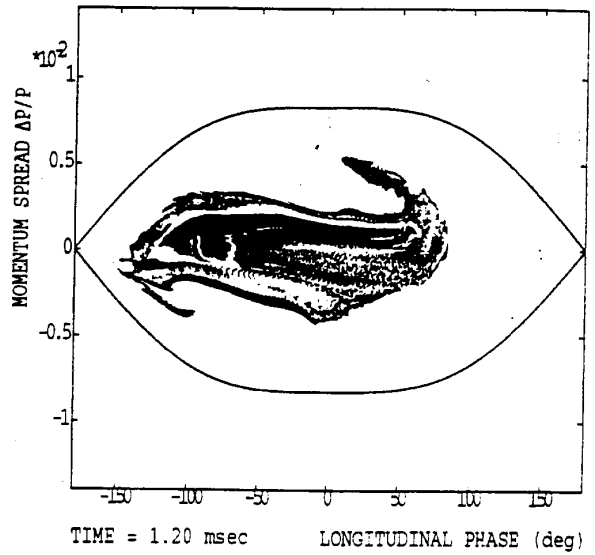
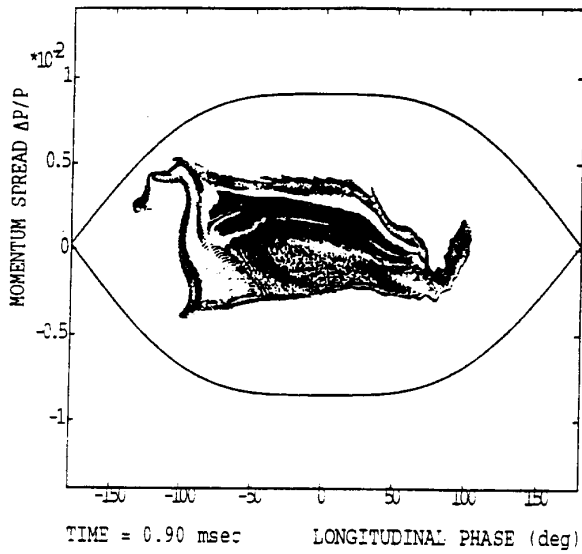
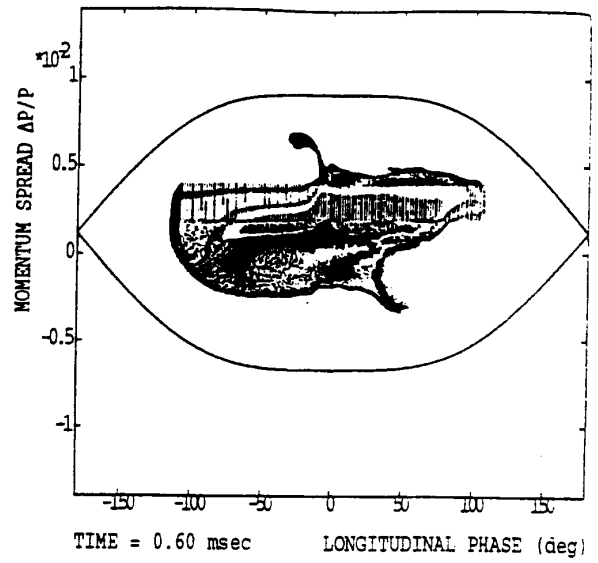
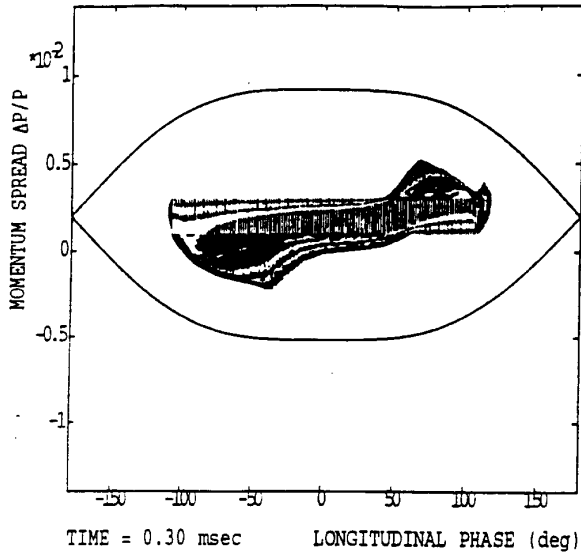
1. F. Jones, "User's Guide to ACCSIM", TRI-DN-90-17, June 1990,
2. C. Prior, "Longitudinal and Transverse Tracking Studies for ESS", in Space Charge Dominated Beams and Applications of High Brightness Beams, S.Y. Lee Editor, AIP Conf. Proceedings, Bloomington, IN., (1995), p. 391.
3. ESS Study: Accumulator Rings and Transport Lines, ESS-96-53-M, 9/96.
4. Sample input deck from C. Prior, The Longitudinal Tracking Code TRACK1D, A Guide for Users. (1996)
5. Lattice output for ESS (private communication).

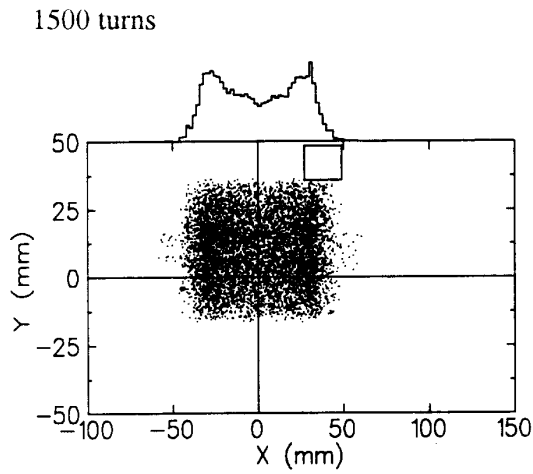
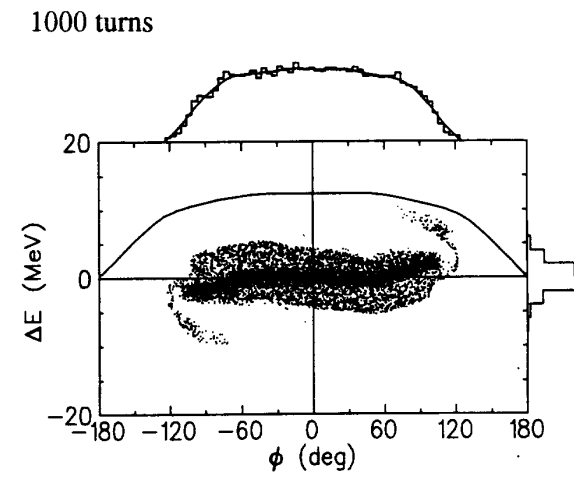
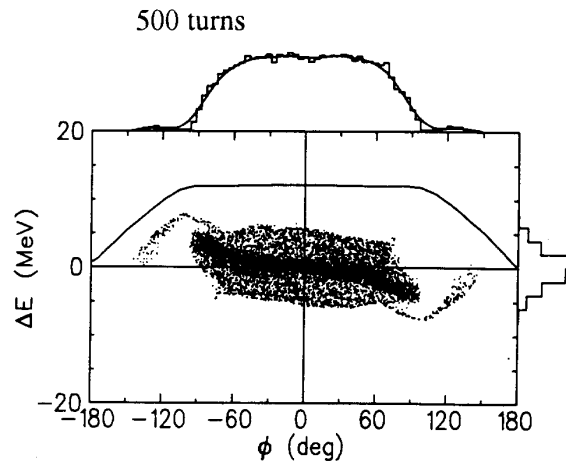
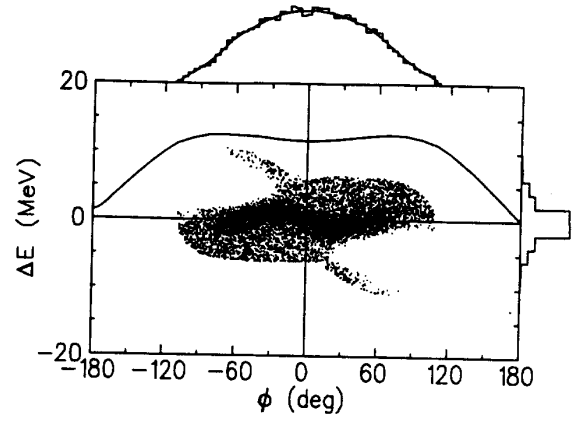
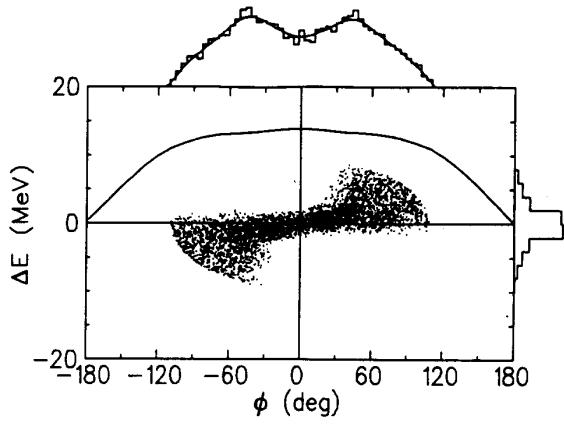
Table 1. Comparison of ESS and SNS Injection Parameters.

	<u>ESS</u>	<u>SNS</u>
Injection energy (GeV)	1.334	1.0
β	0.907	0.875
γ	2.42	2.07
Ring circumference (m)	163.4	220.7
Injection turns	1000	1225
Storage turns after injection	1000	0
Revolution time (ns)	605	842
Chopping fraction	0.60	0.65
ΔE inject (MeV)	1.1 ^(a)	1.0
Injected particles ($\times 10^{14}$)	2.34	2.08
Peak RF voltage (kV)	27	42
Ω_{sync} s ⁻¹ (at peak RF voltage)	1860	2070
X injection painting	with dispersion	bump magnets
Y-injection painting	bump magnets	bump magnets

a - corresponds to $\delta p/p = 0.1\%$

Figure 1. ESS LONGITUDINAL INJECTION, FROM REF. 3.





Transverse @ 2000 turns

Figure 2a. ESS Injection with constant energy, frequency and RF Voltage.

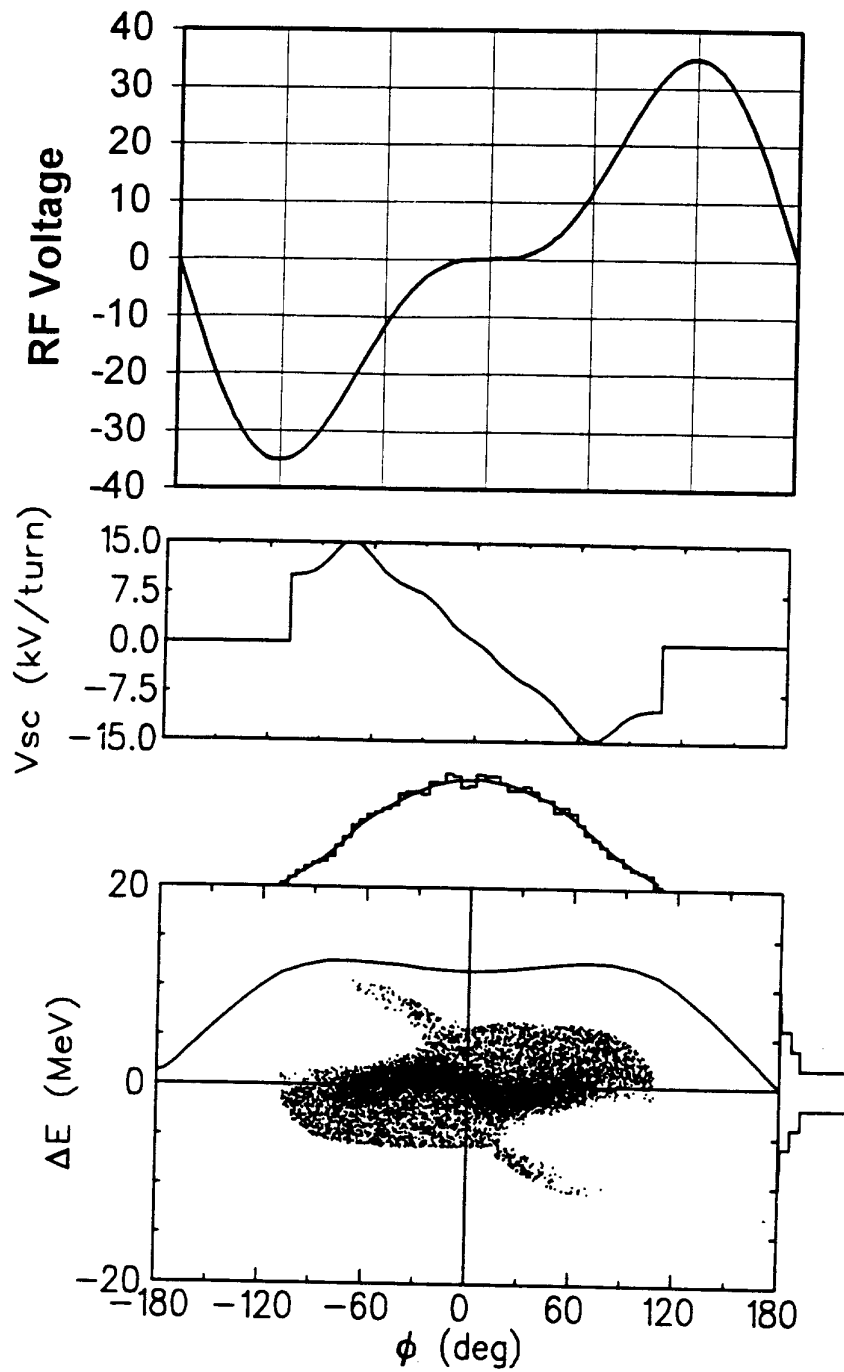
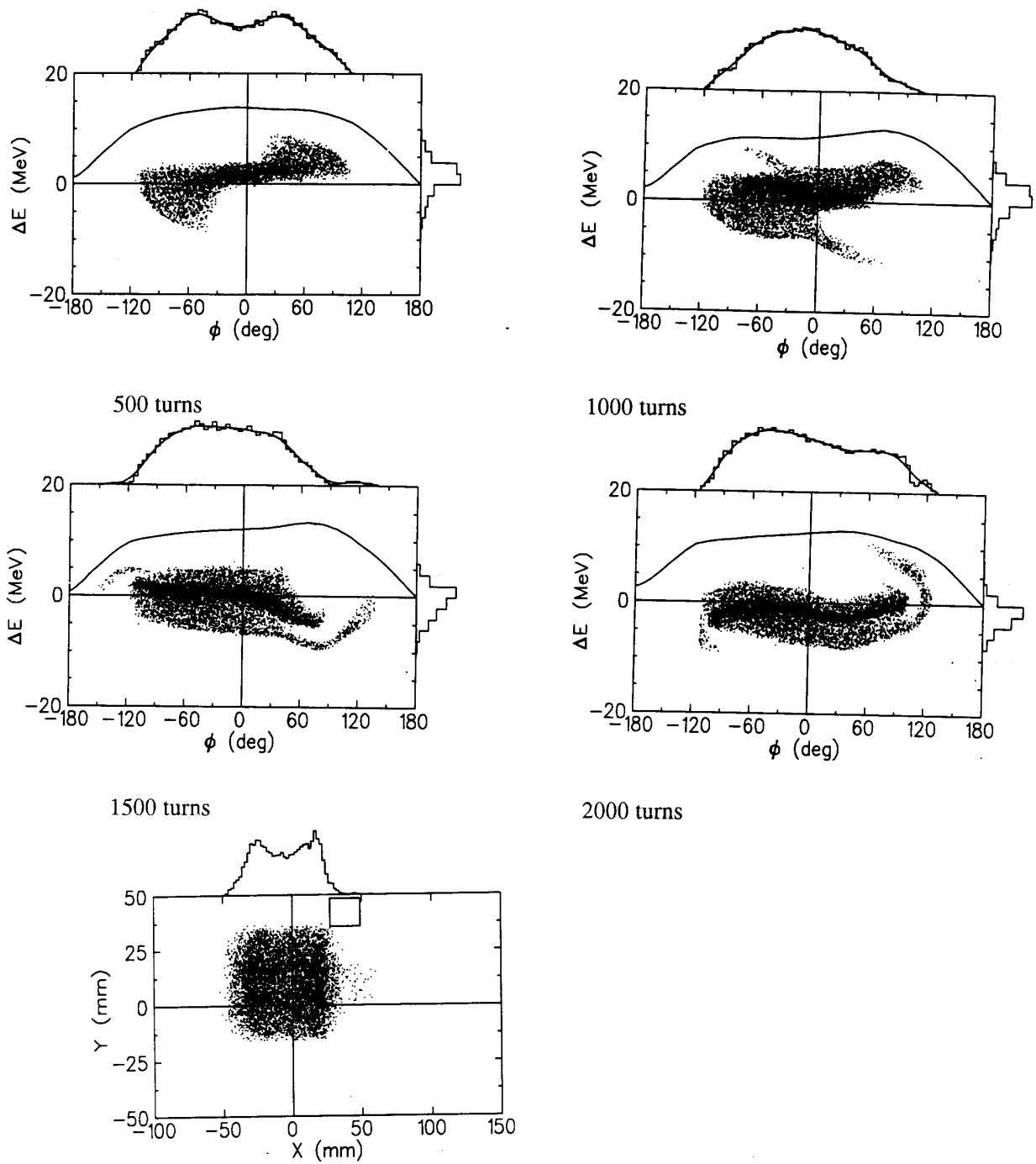


Figure 2b. RF and longitudinal space charge voltages for the case shown in Figure 2, at 1000 turns.



Transverse @ 2000 turns

Figure 3. ESS injection with ramped energy and constant frequency and RF voltage.

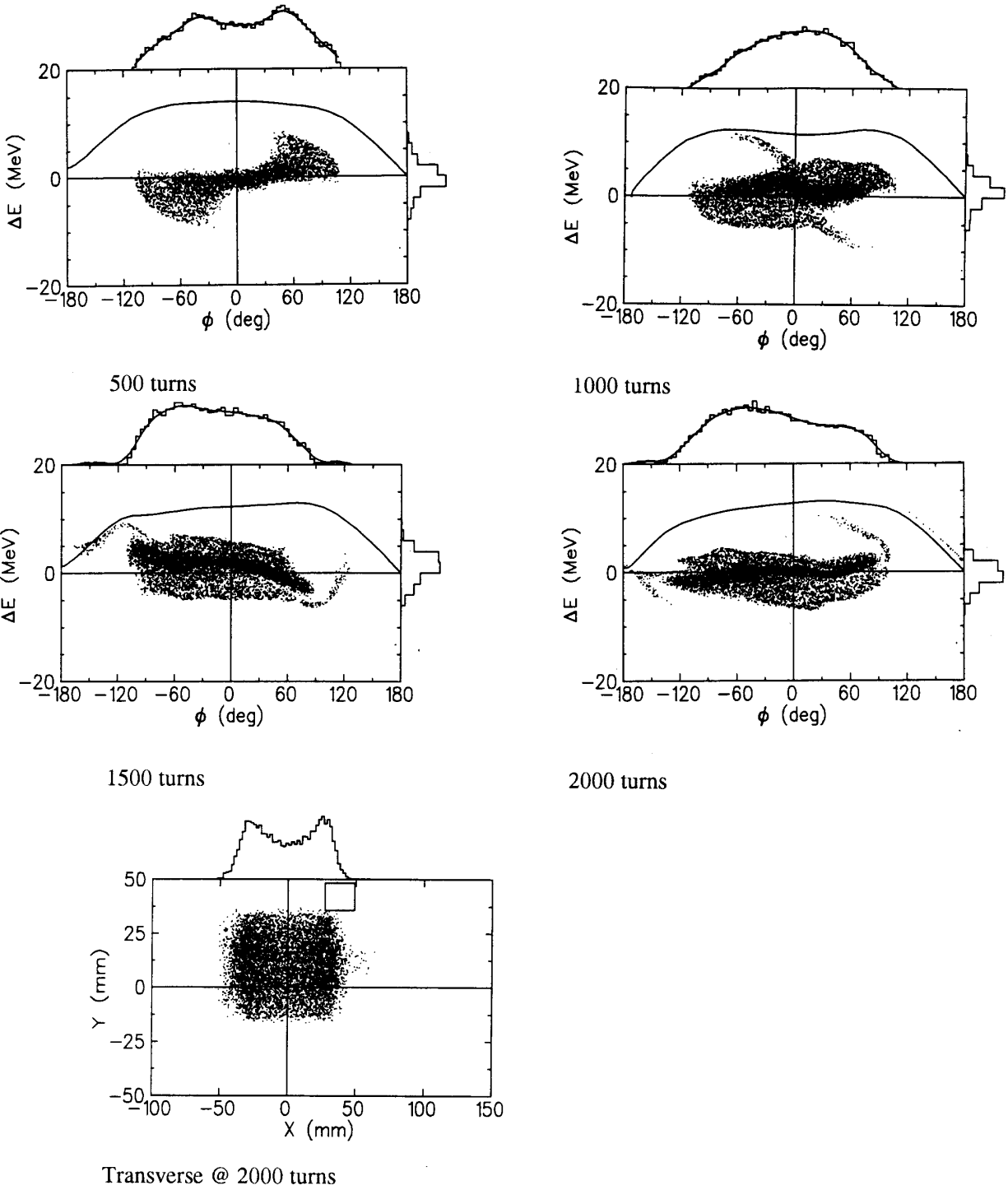


Figure 4. ESS injection with ramped energy and frequency and constant RF voltage.

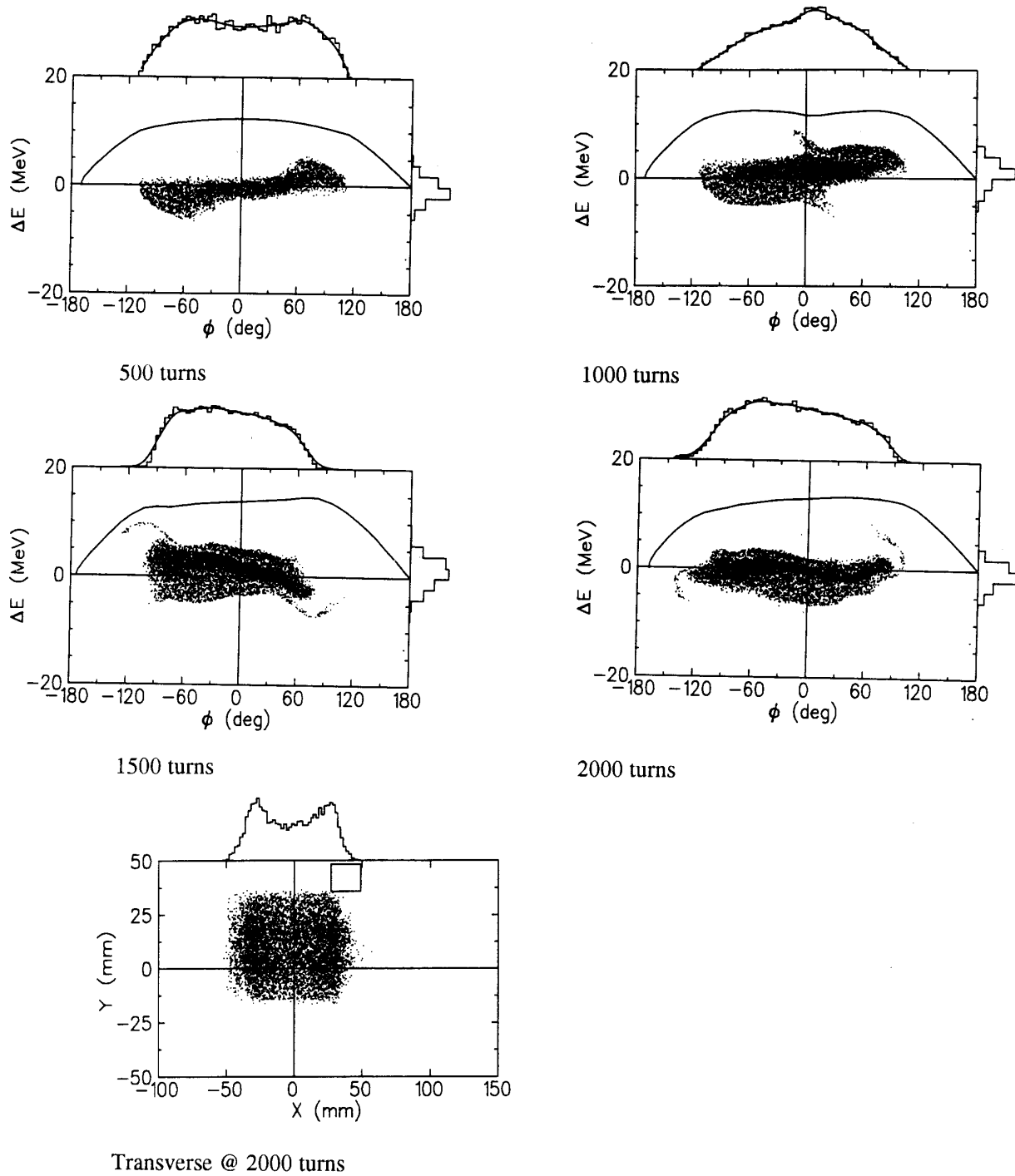
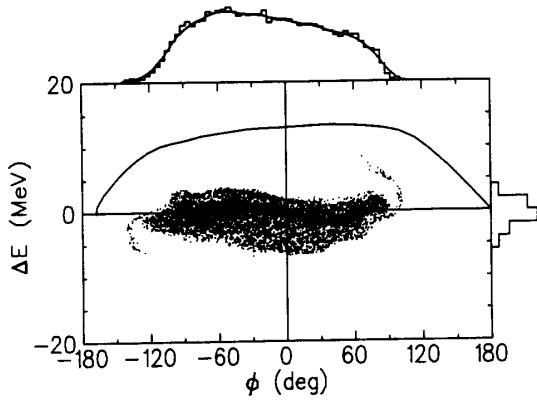
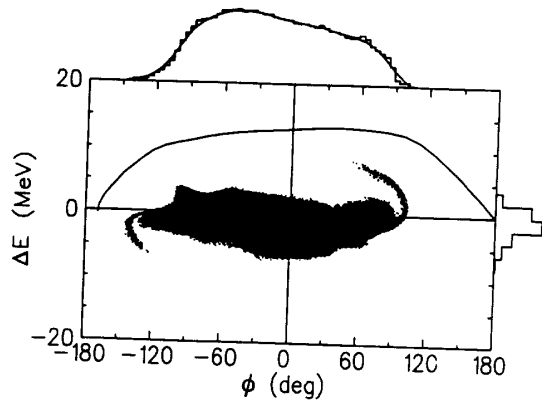


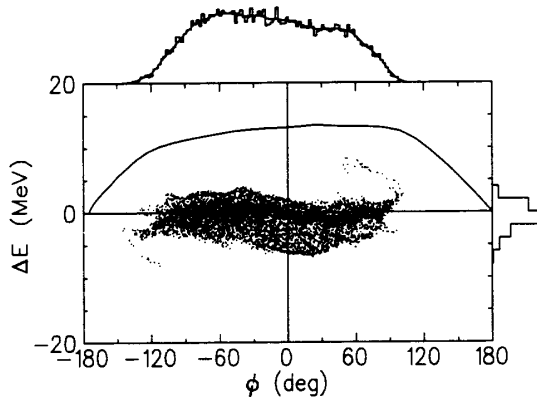
Figure 5. ESS injection with ramped energy, RF frequency and RF voltage.



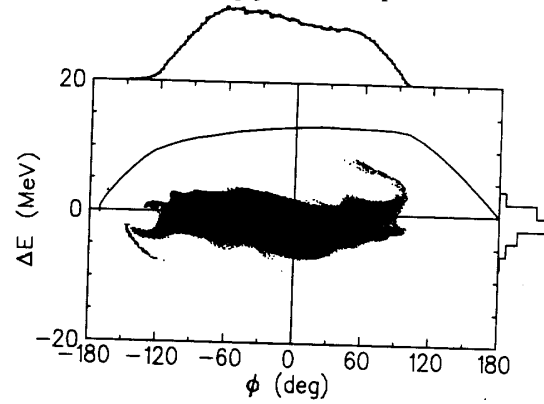
80 bins, 2 smoothing passes, 10^4 particles



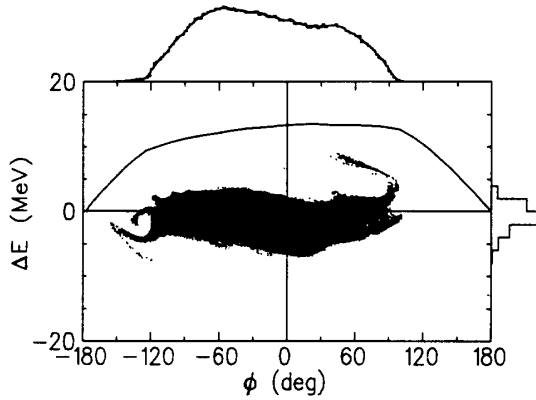
80 bins, 2 smoothing passes, 10^5 particles



160 bins, 2 smoothing passes, 10^4 particles



160 bins, 2 smoothing passes, 10^5 particles



160 bins, 1 smoothing pass, 10^5 particles

Figure 6. Sensitivity of final ESS longitudinal distribution to number of bins, smoothing passes and injected particles .

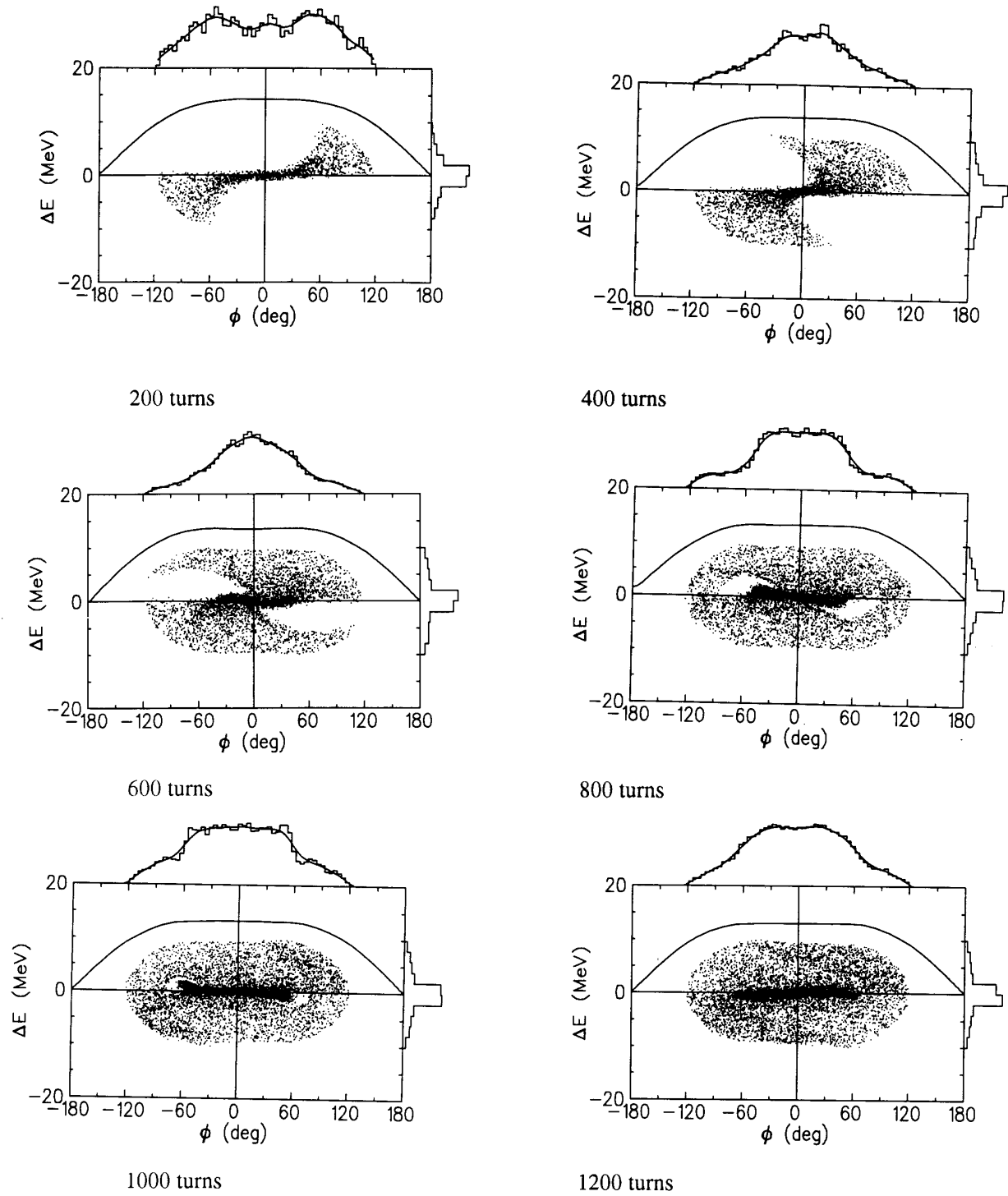


Figure 7. Longitudinal distributions for a typical SNS injection case. Injection occurs over 1225 turns, and the peak RF voltage is 42 kV.

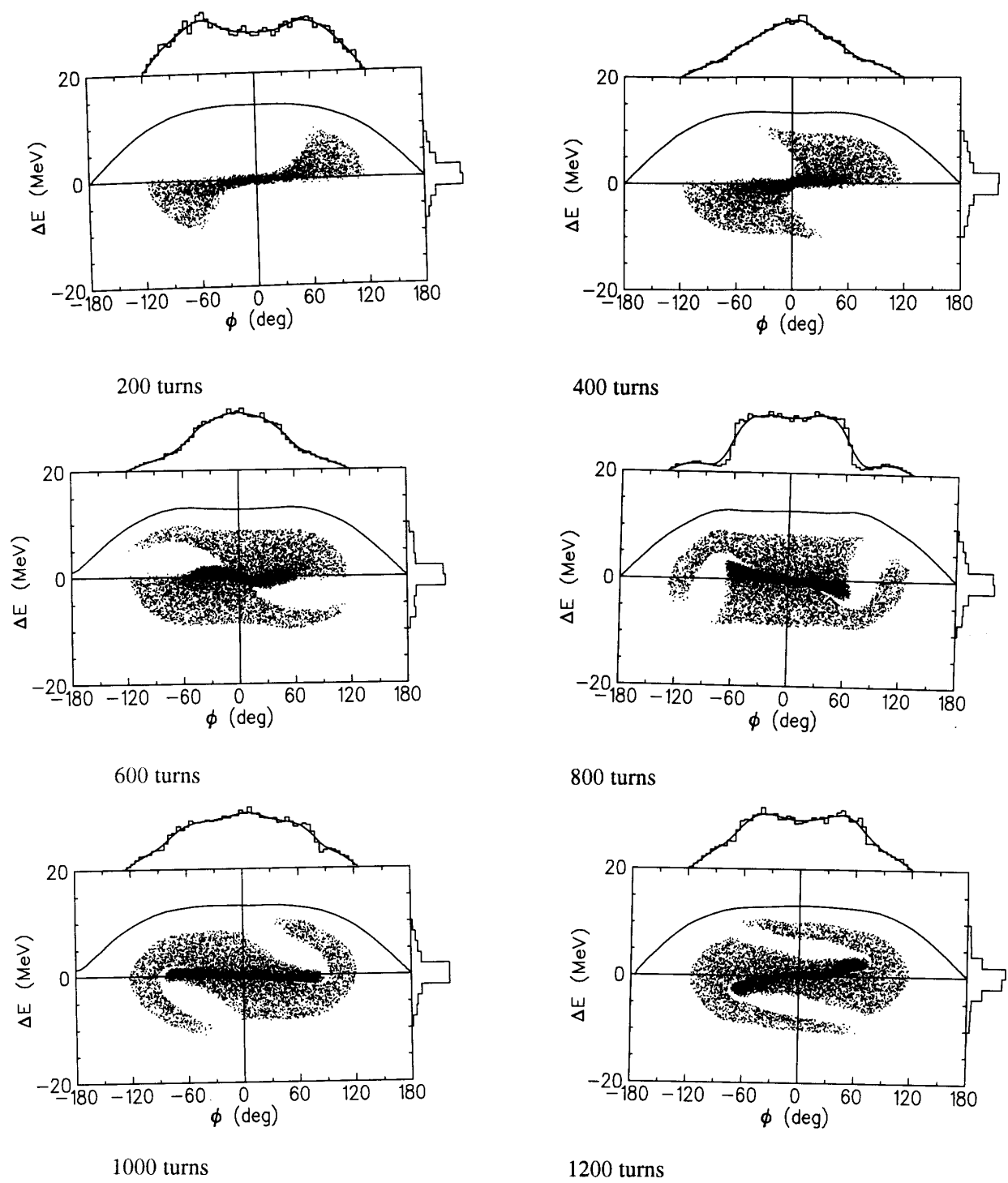


Figure 8. Longitudinal distributions for an SNS case where injection occurs over 612 turns and the particles are then held the remaining 613 turns. The peak RF voltage is 42 kV.

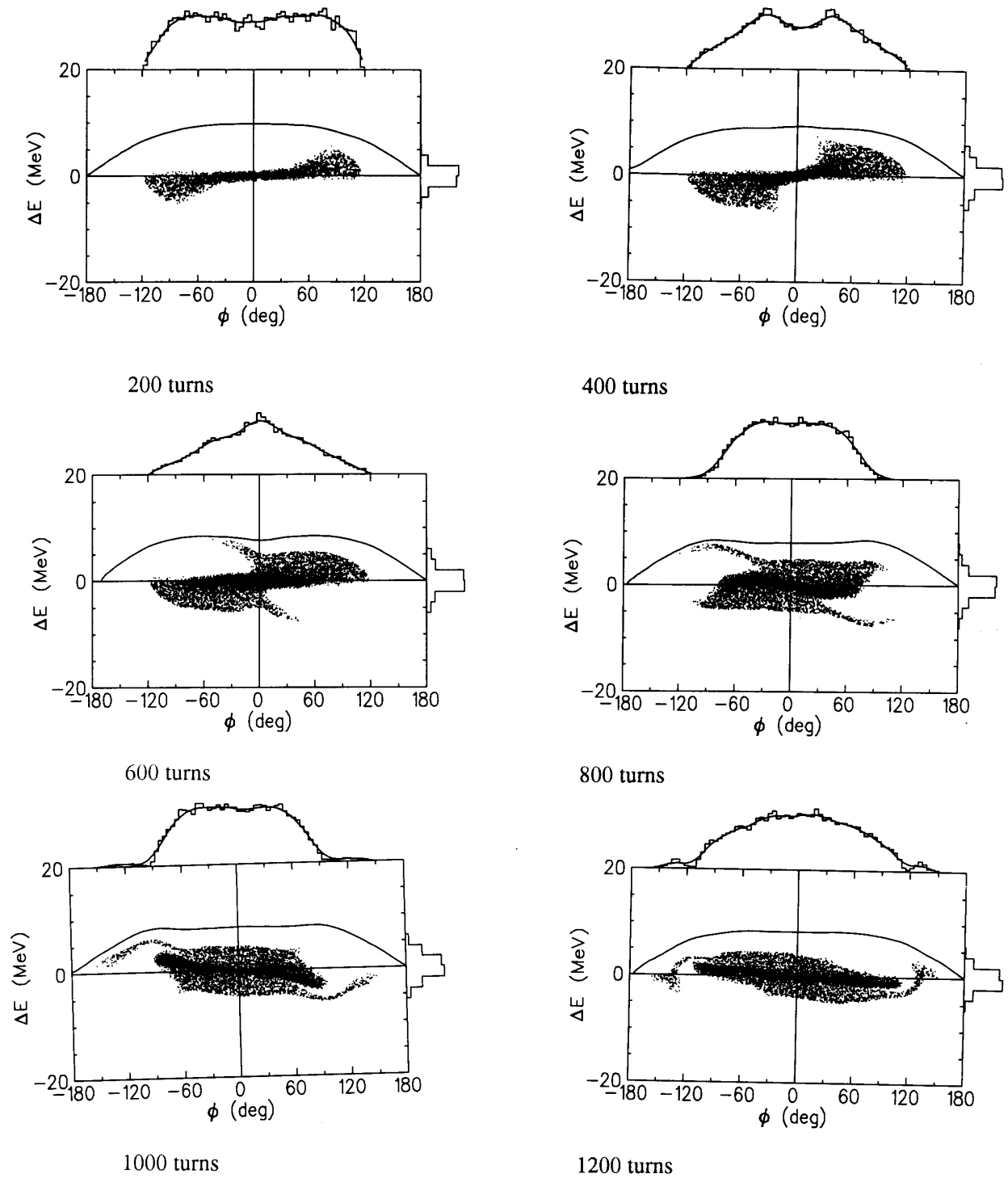


Figure 9. Longitudinal distributions for an SNS case where injection occurs over 612 turns and the particles are then held the remaining 613 turns and t peak RF voltage is 21 kV.